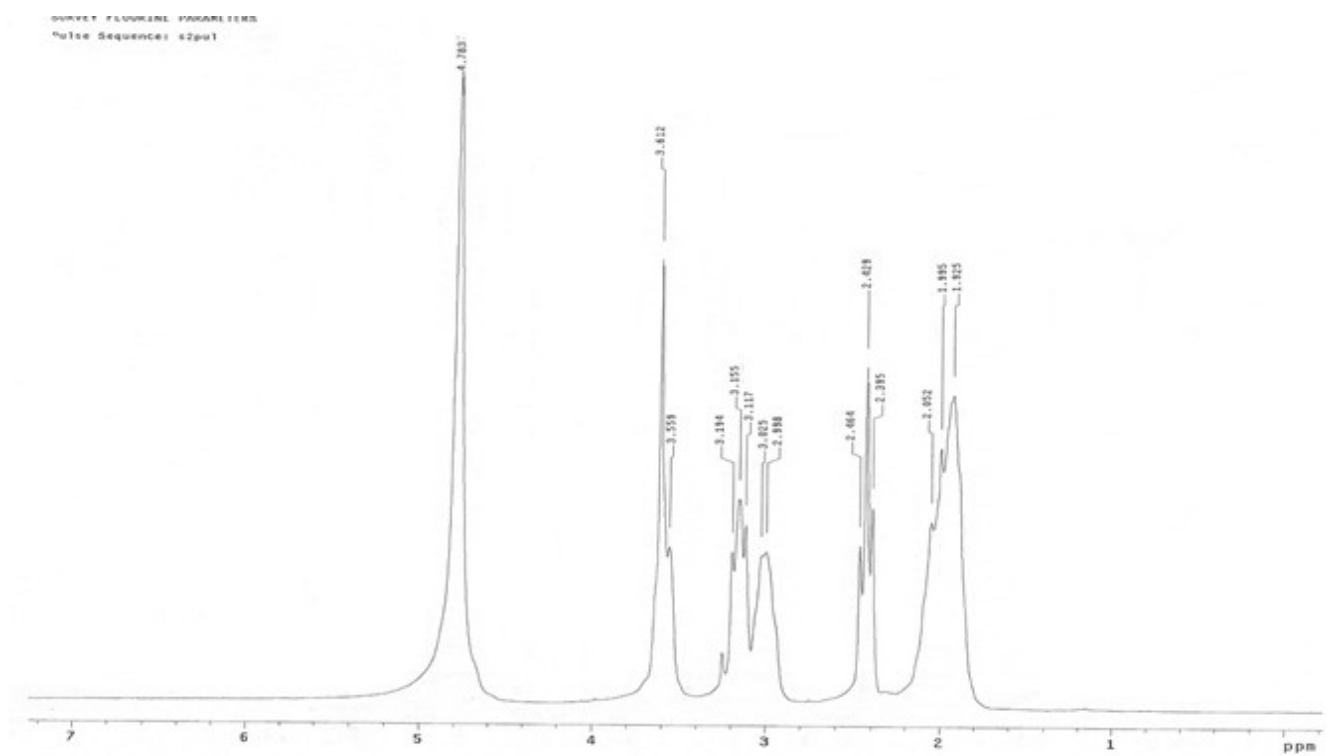
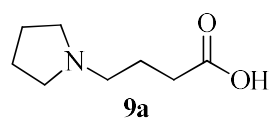


## **Supplementary Information**

Erika Tovar-Gudiño<sup>1</sup>, Juan Alberto Guevara-Salazar <sup>2</sup>, José Raúl Bahena-Herrera <sup>3</sup>, José Guadalupe Trujillo-Ferrara <sup>2</sup>, Zuleyma Martínez-Campos <sup>1</sup>, Rodrigo Said Razo-Hernández <sup>3</sup>, Angel Zamudio <sup>3</sup>, Nina Pastor <sup>3</sup>, Mario Fernández-Zertuche <sup>1\*</sup>

Figure S1	2
Figure S2	3
Figure S3	4
Figure S4	5
Figure S5	6
Figure S6	7
Figure S7	8
Figure 8S	9
Figure S9	10
Figure S10	11
Figure S11	12
Figure S12	13
Figure S13	14
Figure S14	15
Figure S15	16
Figure S16	17
Figure S17	17
Figure S18	18
Figure S19	19
Figure S20	20
Figure S21	21
Figure S22	22
Table S1	22
Figure S23	23
Figure S24	25
Figure S25	26
Table S2	26
Figure S26	27
Figure S27	28



**Figure S1.**  $^1\text{H}$  NMR ( $\text{D}_2\text{O}$ , 200 MHz) of 4-(Pyrrolidin-1-yl)butanoic acid (**9a**).

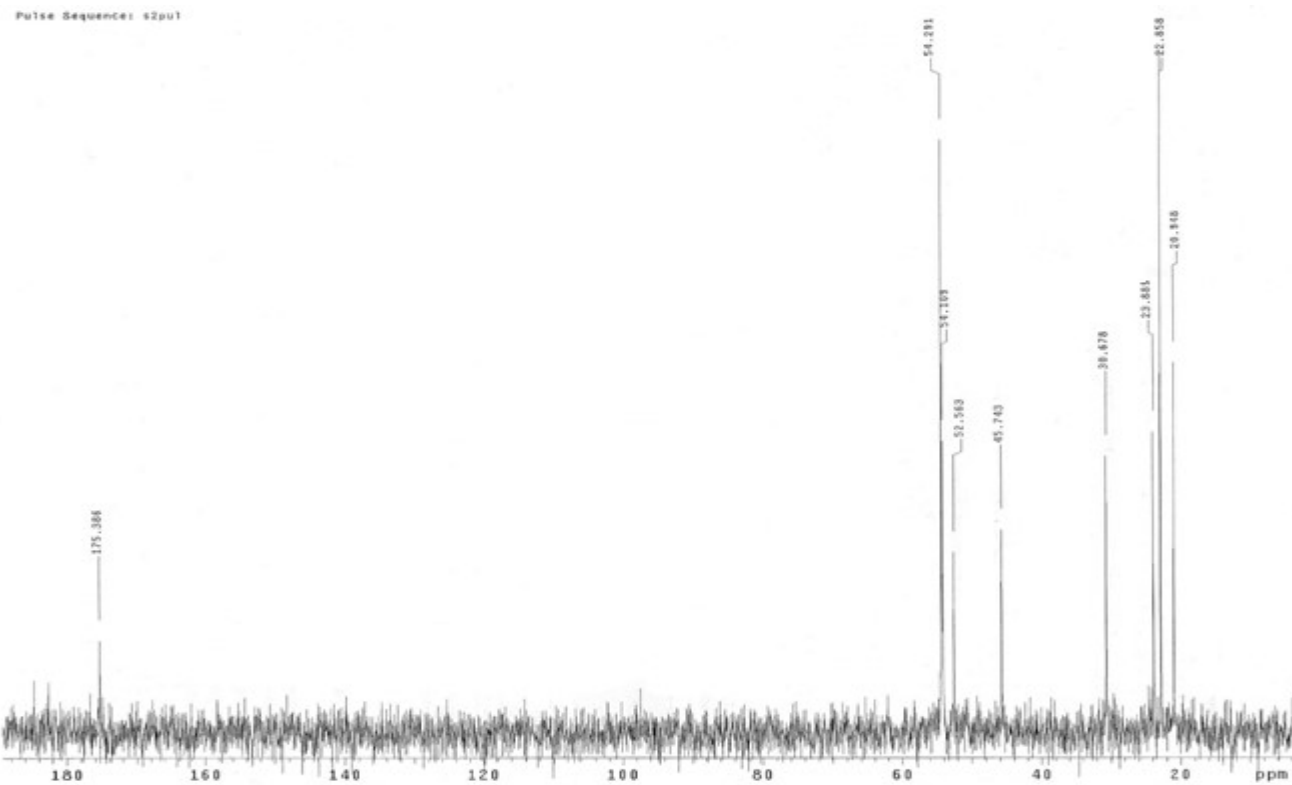
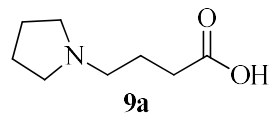


**Figure S2.**  $^{13}\text{C}$  NMR ( $\text{D}_2\text{O}$ , 200 MHz) of 4-(Pyrrolidin-1-yl)butanoic acid (**9a**).

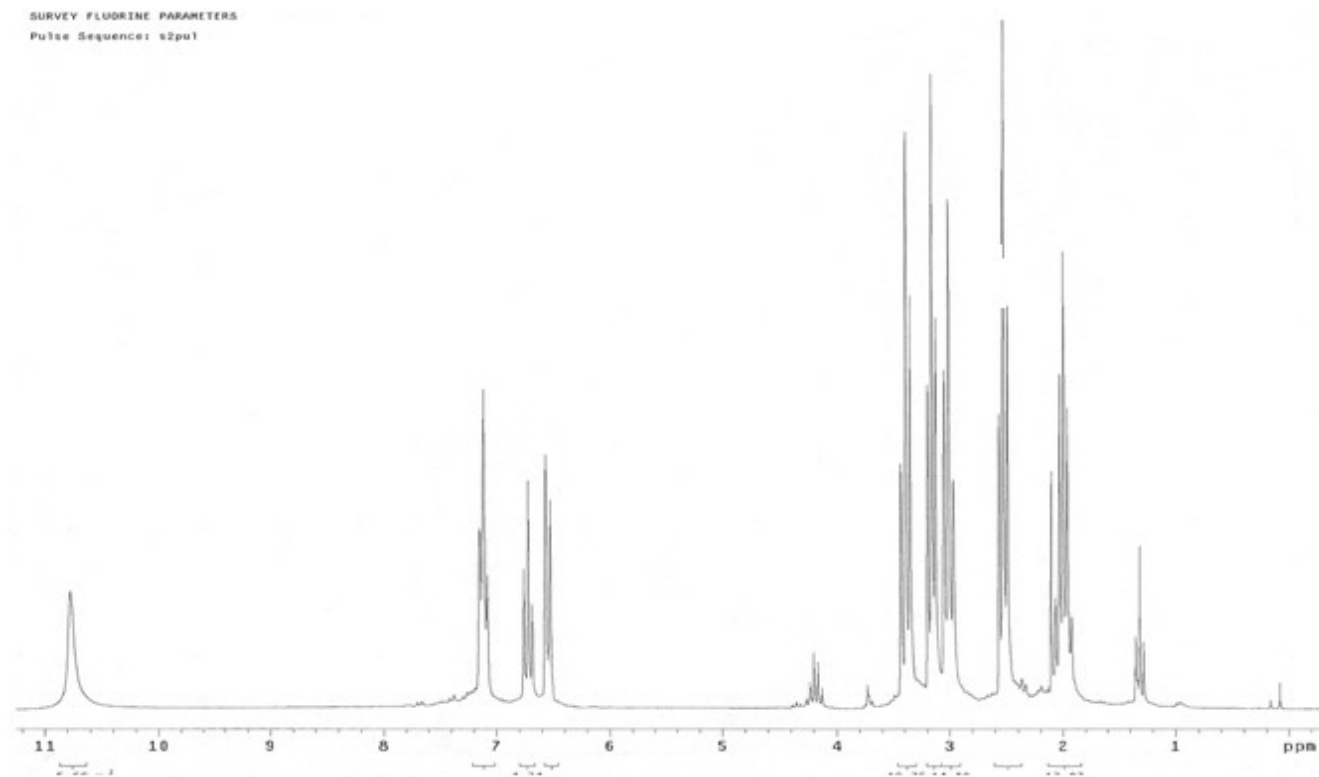
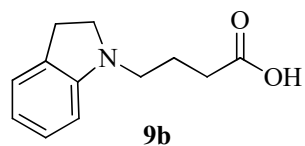


**Figure S3.**  $^1\text{H}$  NMR ( $\text{CDCl}_3$ , 200 MHz) of 4-(Indolin-1-yl)butanoic acid (**9b**).

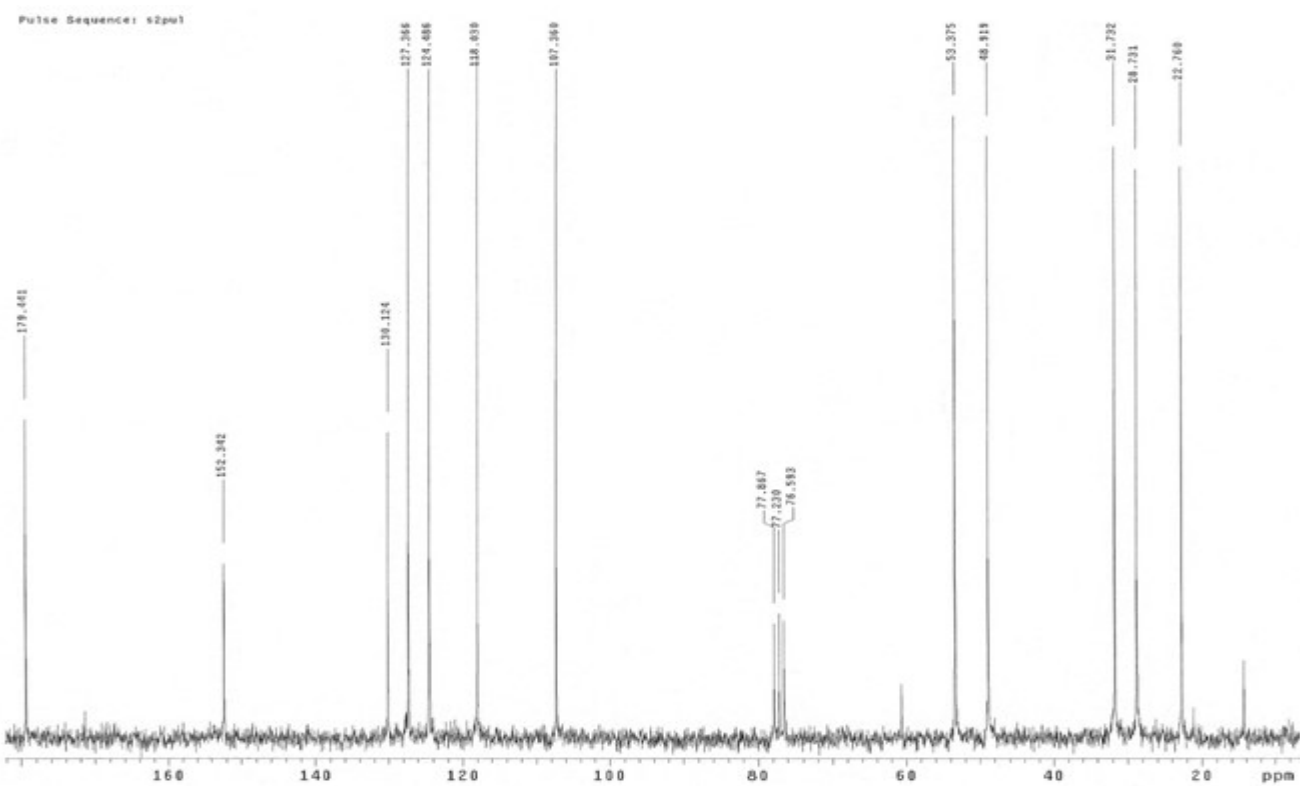
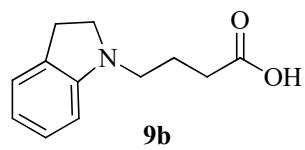


**Figure S4.**  $^{13}\text{C}$  NMR ( $\text{CDCl}_3$ , 200 MHz) of **4-(Indolin-1-yl)butanoic acid (9b)**.

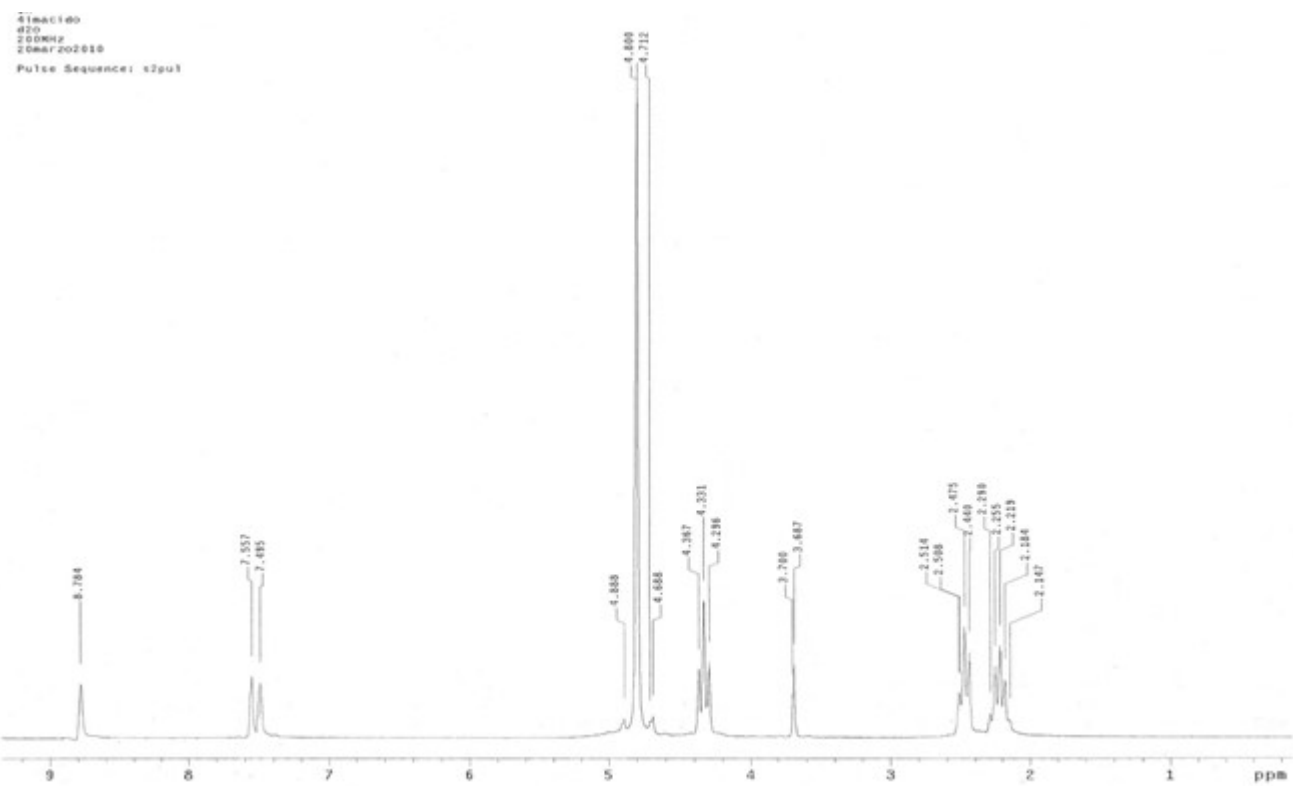
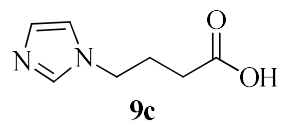


**Figure S5.**  $^1\text{H}$  NMR ( $\text{D}_2\text{O}$ , 200 MHz) of **4-(1H-Imidazol-1-yl)butanoic acid (9c)**.

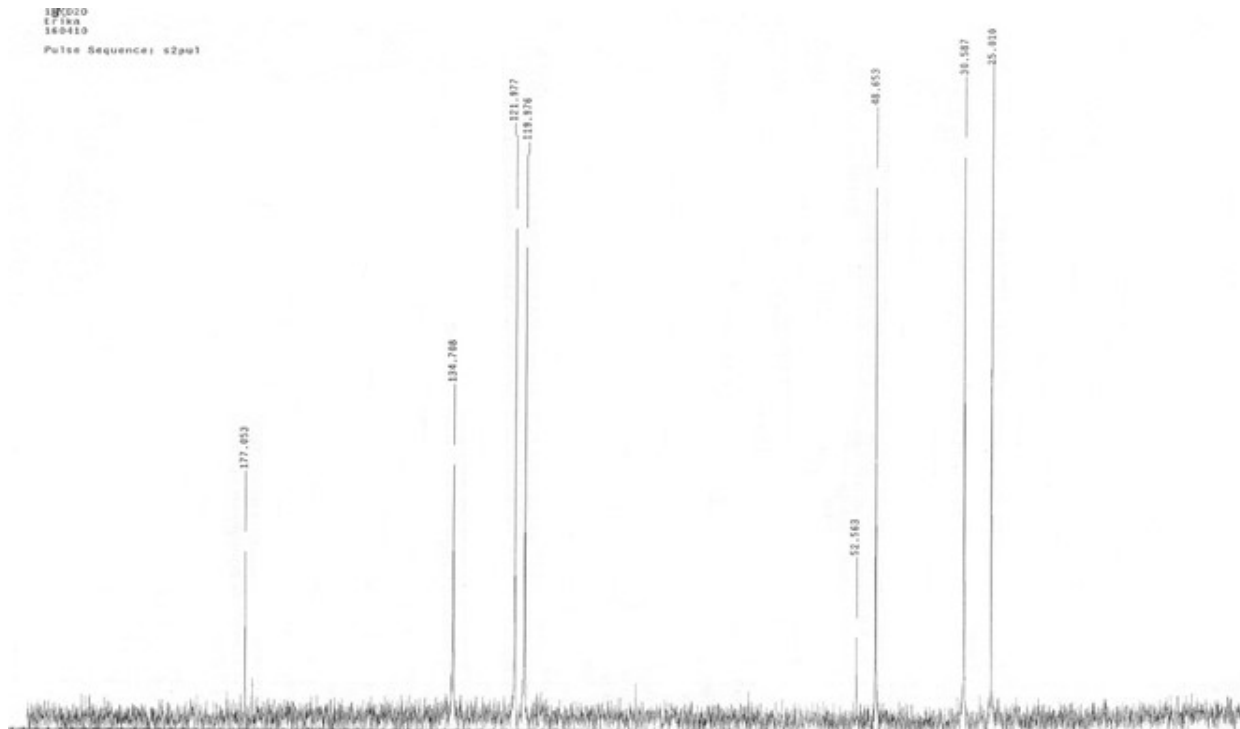
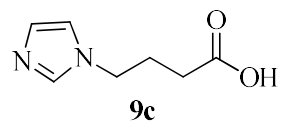


**Figure S6.**  $^{13}\text{C}$  NMR ( $\text{D}_2\text{O}$ , 200 MHz) of **4-(1H-Imidazol-1-yl)butanoic acid (9c)**.

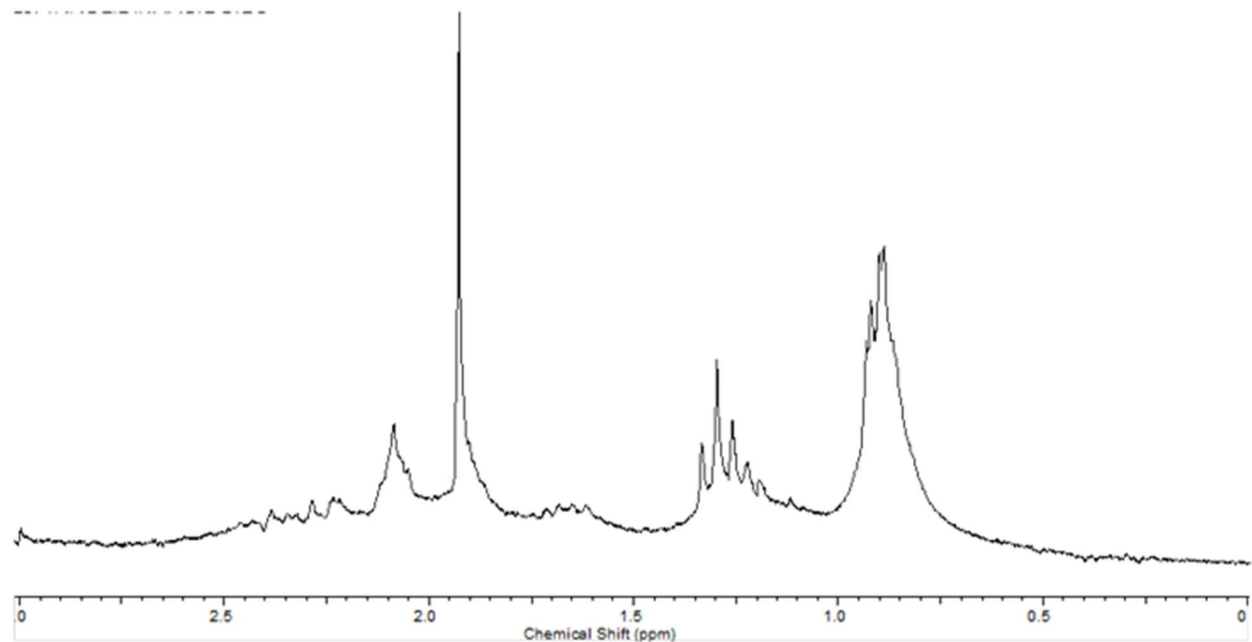
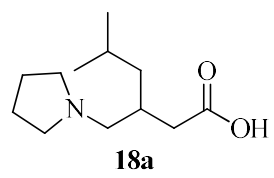


**Figure S7.** <sup>1</sup>H NMR ( $D_2O$ , 200 MHz) of 5-methyl-3-(pyrrolidin-1-ylmethyl)hexanoic acid (18a).

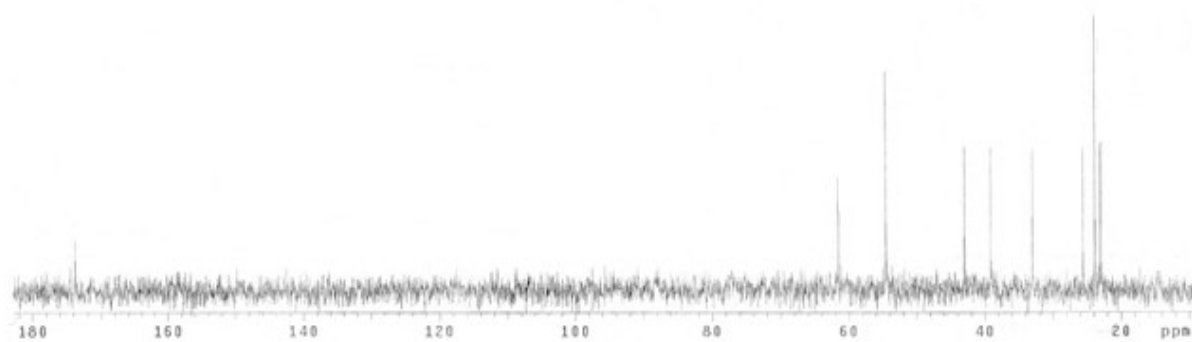
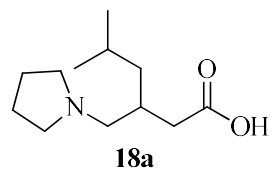


**Figure S8.**  $^{13}\text{C}$  NMR ( $\text{D}_2\text{O}$ , 200 MHz) of 5-methyl-3-(pyrrolidin-1-ylmethyl)hexanoic acid (**18a**).

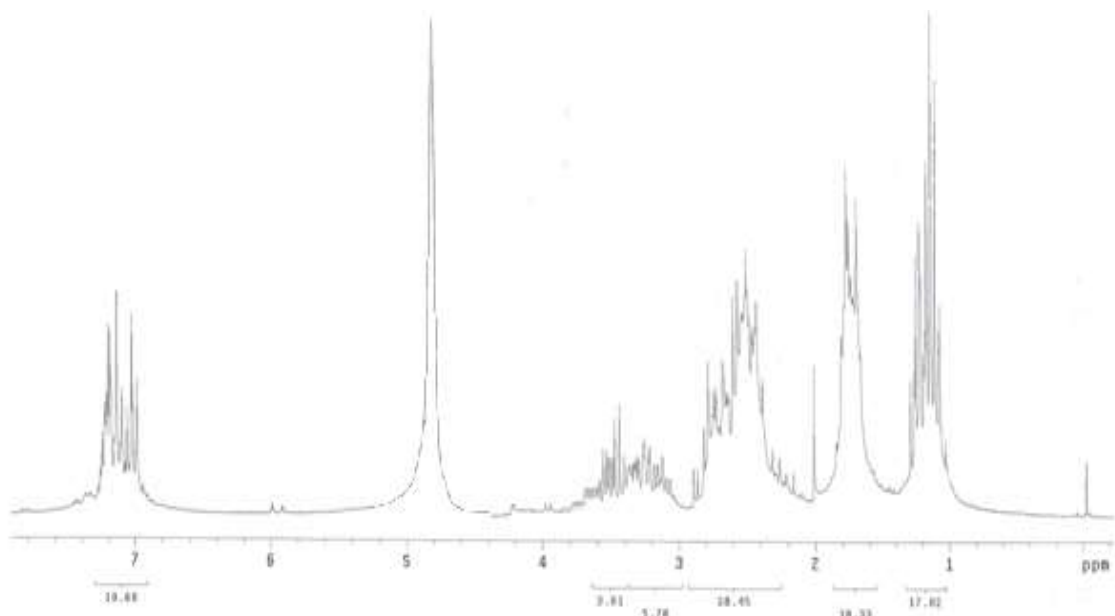
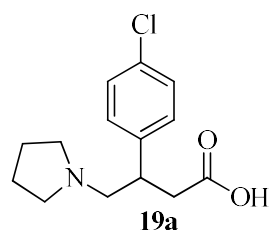


**Figure S9.**  $^1\text{H}$  NMR ( $\text{D}_2\text{O}$ , 200 MHz) of 3-(4-chlorophenyl)-4-(pyrrolidin-1-yl)butanoic acid (19a).

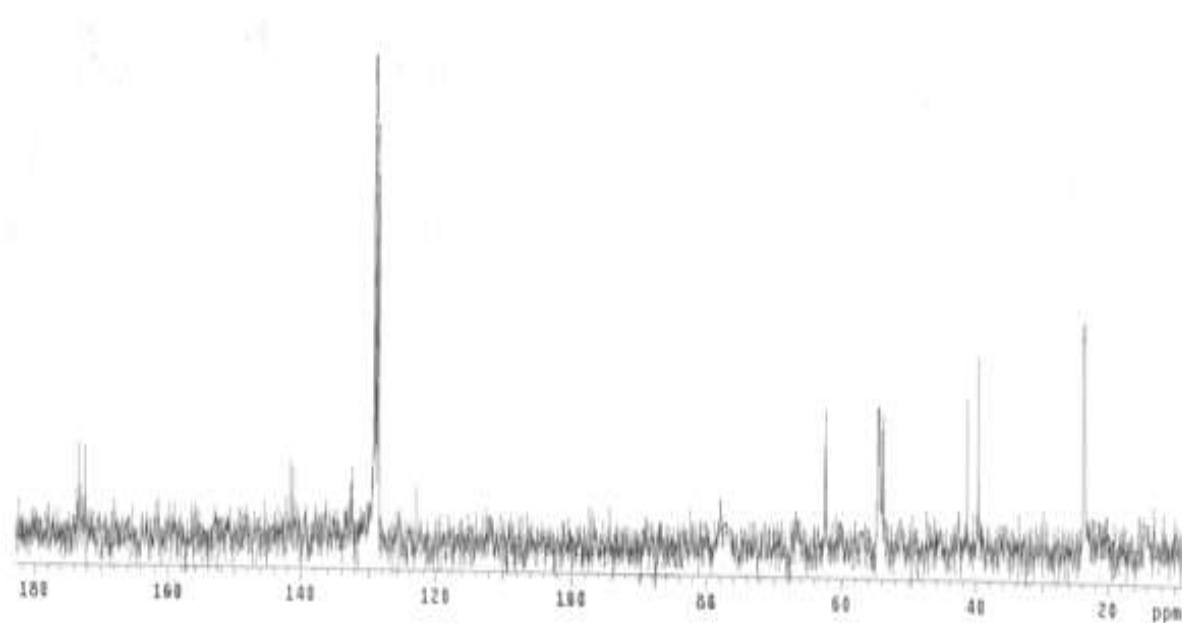
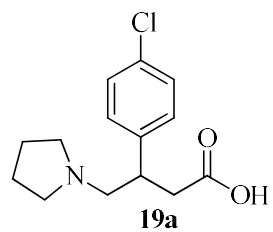


**Figure S10.** <sup>13</sup>C NMR ( $\text{D}_2\text{O}$ , 200 MHz) of 3-(4-chlorophenyl)-4-(pyrrolidin-1-yl)butanoic acid (**19a**).

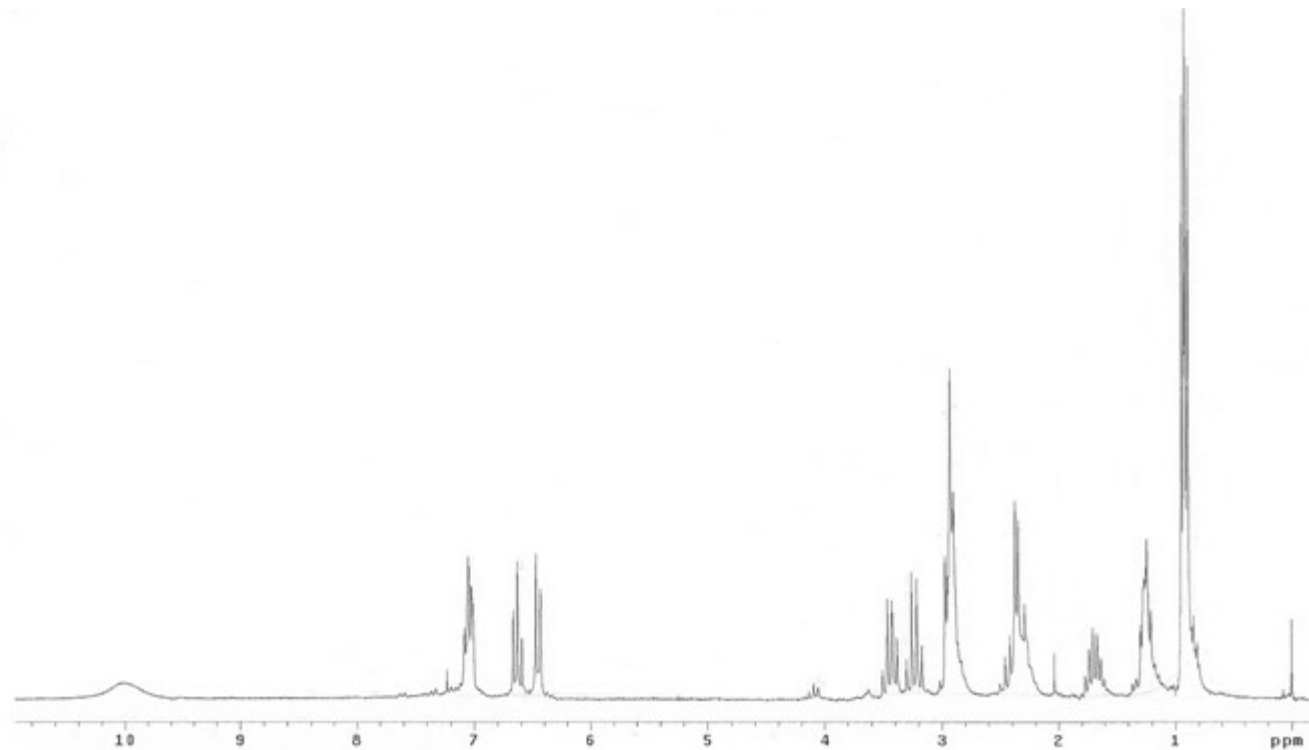
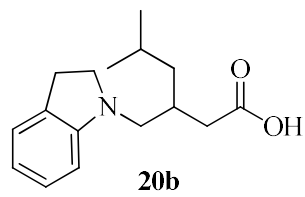


**Figure S11.**  $^1\text{H}$  NMR ( $\text{CDCl}_3$ , 200 MHz) of 3-(Indolin-1-ylmethyl)-5-methylhexanoic acid (**20b**).

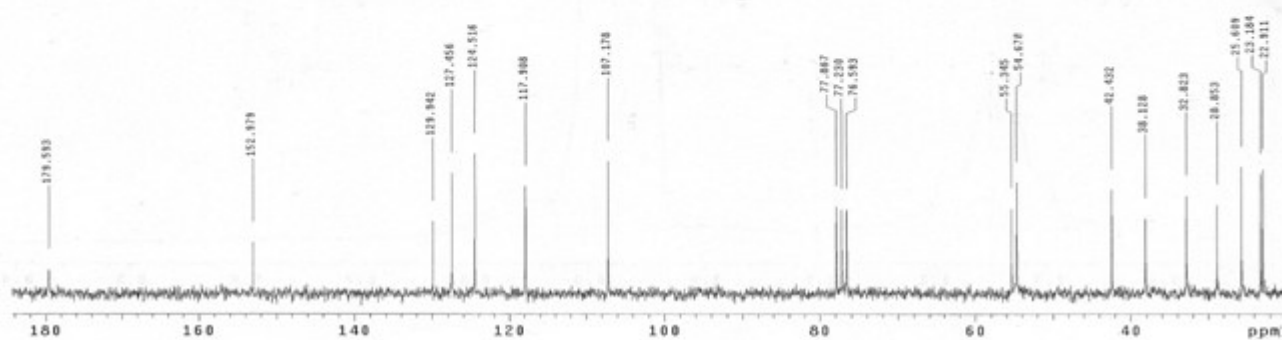
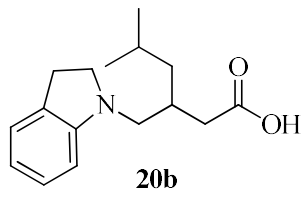
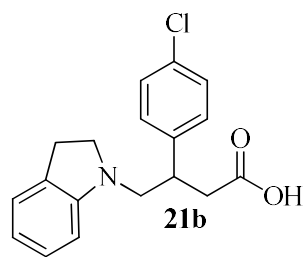


**Figure S12.**  $^{13}\text{C}$  NMR ( $\text{CDCl}_3$ , 200 MHz) of 3-(Indolin-1-ylmethyl)-5-methylhexanoic acid (20b).



15abril2013pClindolinaacido1Hcdcl3good

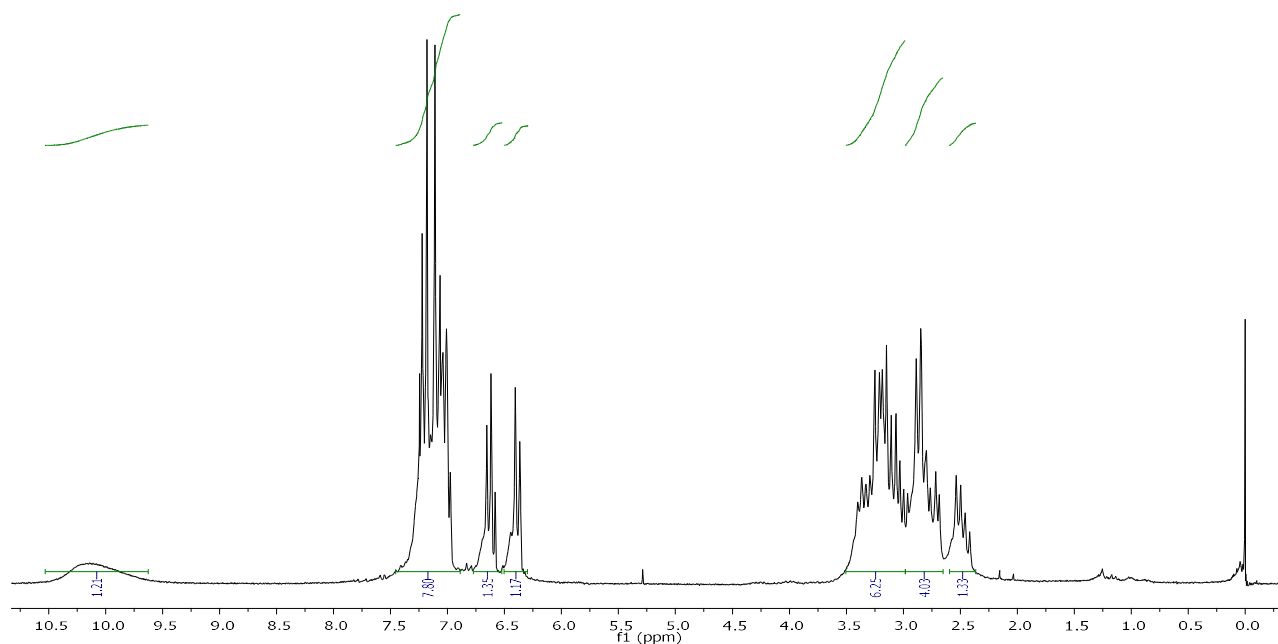


**Figure S13.**  $^1\text{H}$  NMR ( $\text{CDCl}_3$ , 200 MHz) of 3-(4-Chlorophenyl)-4-(indolin-1-yl)butanoic acid (21b).

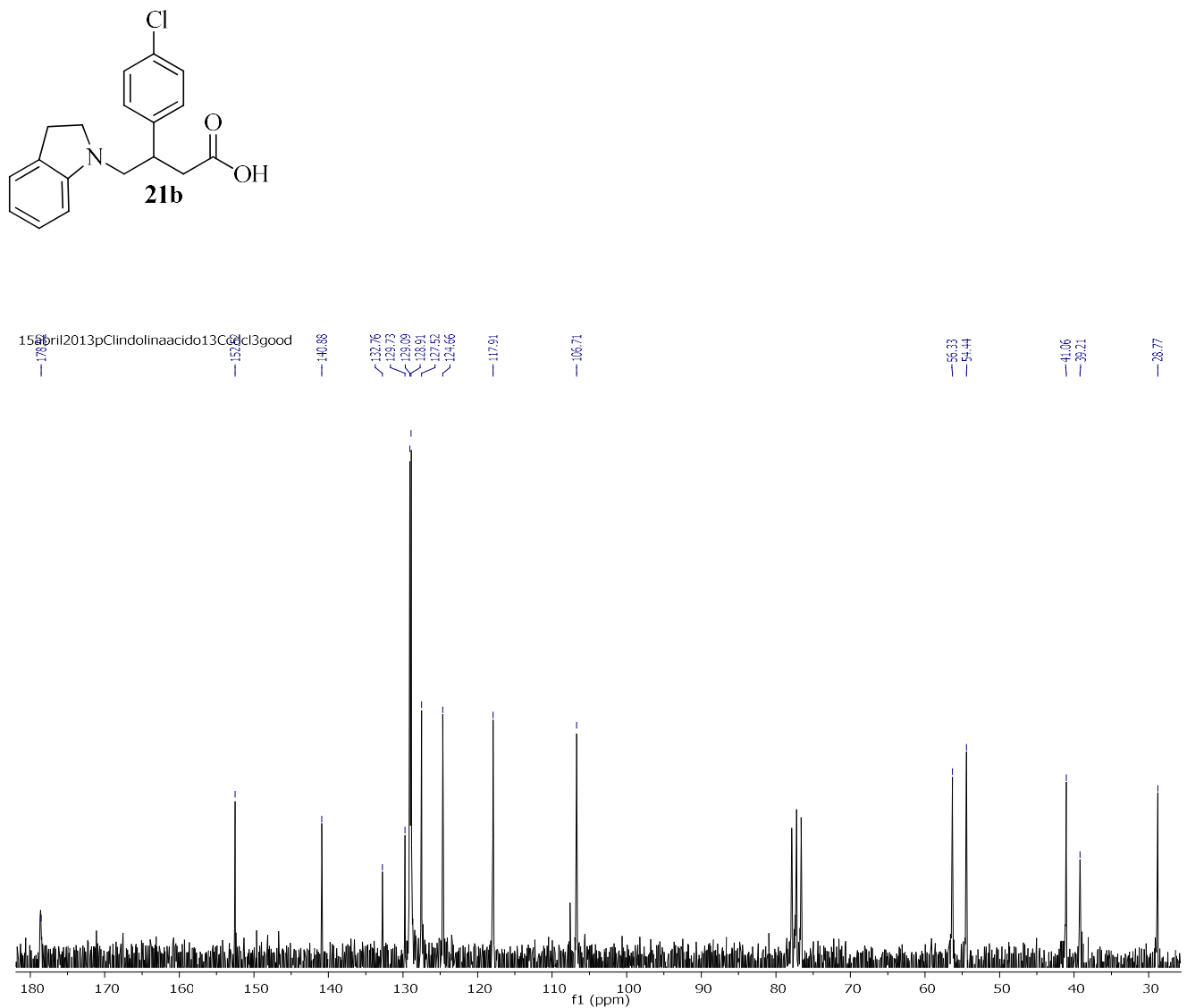


**Figure S14.** <sup>13</sup>C NMR (CDCl<sub>3</sub>, 200 MHz) of **3-(4-Chlorophenyl)-4-(indolin-1-yl)butanoic acid (21b)**.

PF	-----MSNKTNASLMKRREAAVPRGVGQIHP-IFAESAKNATVTDVEGREFIG
EC	-----NSNKELMQRRSQAI PRGVGQIHP-FADRAENCRVWDVEGREYLD
HS	-FDYDGPLMKTEVPGPRSQUELMQLNII--QNAEAVHFFCNYEESRGNYLVDVDGNRMLD
JB	-FDYDGPLMKTEVPGPRSQUELMQLNII--QNAEAVHFFCNYEESRGNYLVDVDGNRMLD
PF	FAGGI AVLNTGHLHPKIIIAAVTEQLNKLTH---TCFQVLAYEPYVELCEKVNAK-VPGDF
EC	FAGGI AVLNTGHLHPKVVAAVEAQLKKLSH---TCFQVLAYEPYLELCEI-MNQKVPGDF
HS	LYSQISSPIGYSHPALLKLIQQPQNAMFVNRPALGILPPENFVEKLRQSLLSVAPKGM
JB	LYSQISSPIGYSHPALVKLVQQPQNVSTFINRPALGILPPENFVEKLRQSLLSVAPKGM
PF	AKKTLLVTTGSEA-----VENAVKIARATTGRAGVIAFT
EC	AKKTLLVTTGSEAVENA-----VKIARAATKRSGTIAFS
HS	-SQLITMACGSCSNENALKTI FMWYRSKERGQRGFSQEELET CMINQAPGCPDYSI LSF M
JB	-SQLITMACGSCSNENAFKTI FMWYRSKERGESAFSKEELET CMINQAPGCPDYSI LSF M
PF	GAYHGRTMMLTGLTGKVV PYSAGMGLM--P-GGIFRALYPNELHGVS-V---DDSIAS-I
EC	GAYHGRTHYTALTGKVN PYSAGMGL--MPGHVYRALYPCPLHGI---SEDDAIASI-
HS	GAFHGRTMGCLATTHSKAIHKIDIPSFDWIAPFPRLKYPLEEFVKENQQEEARCLEEV E
JB	GAFHGRTMGCLATTHSKAIHKIDIPSFDWIAPFPRLKYPLEEFVKENQQEEARCLEEV E
PF	ERIFKNDAEPRDIAIIIEPVQGE GGFYVAPKA FMKRLRELCDKHGILLIADEV QTGAGR
EC	HRIFKNDAAPE DIAIIIVIEPVQGE GGFYASSPAFMQRRLRALCDEHGI MLIADEV QSGAGR
HS	DLIVKYRKKKTVAGIIVEPIQSEG GDNHASDDFRKLRDIARKHGAFLVDEV QTGGC
JB	DLIVKYRKKKTVAGIIVEPIQSEG GDNHASDDFRKLRDISRKHGAFLVDEV QTGGGS
PF	TGTFFAMEQM GVAA--DLTTFA KSI-AGGFPLAGVCGKA EYMDA IAPGGL GGT YAGSPIA
EC	TGTLFAMEQM GVAP--DLTTFA KSI-AGGFPLAGVTGRAEVMDA VAPGGL GGT YAGNPIA
HS	TGKFWAHEHWGLDDP ADVMTFS KKMMTGGFFH----K-EEFRPNAPYRI FNT WLGDP SK
JB	TGKFWAHEHWGLDDP ADVMTFS KKMMTGGFFH----K-EEFRPNAPYRI FNT WLGDP SK
PF	CAAALAVMEV FEEHLLDRCKAVGERLVTGLKAIQAKY PVI-GEVR ALGAMIA LE LFEDG
EC	CVAALEVLKVFQE NLLQKANDLGQKLKDGLL AIAEKHPEI-GDV RGLGAMIA IELFEDG
HS	NLLLAEVINI IKREDLLNNAAHAGK ALLTGLLDLQARYPQFISRV RGRGTFCSFDT---
JB	NLLLAEVINI IKREDLLSNAAHAGK VLLTGLLDLQARYPQFISRV RGRGTFCSFDT---
PF	DSHKPNAAAVASVVA KARDKG LILLSCGT YGNV LRV L VPL TSPD EQLDKGLAIIEECFSEL-
EC	DHNKPDAKLT AEIVAR ARDKGLILLSCGPYY NVL RILVPL TIEDAQIRQGLEI ISQC FDEAK
HS	----PDD SIRNKLILIARNKG VV LGCGDKSIRFRPTLVFRDH HA--HLFLNIFSDILADFK
JB	----PDESIRNKLISIARNKG VMLGGCGDKSIRFRPTLVFRDH HA--HLFLNIFSDILADFK

**Figure S15 .** Alignment of *pseudomonas fluorescens* (PF), *human* (HS), *E. coli* (EC) and *wild boar* (JB). Red and blue color letters corresponds to the residues of the chain A and chain B respectively, that interact with vigabatrin in the 1ohv crystal structure.

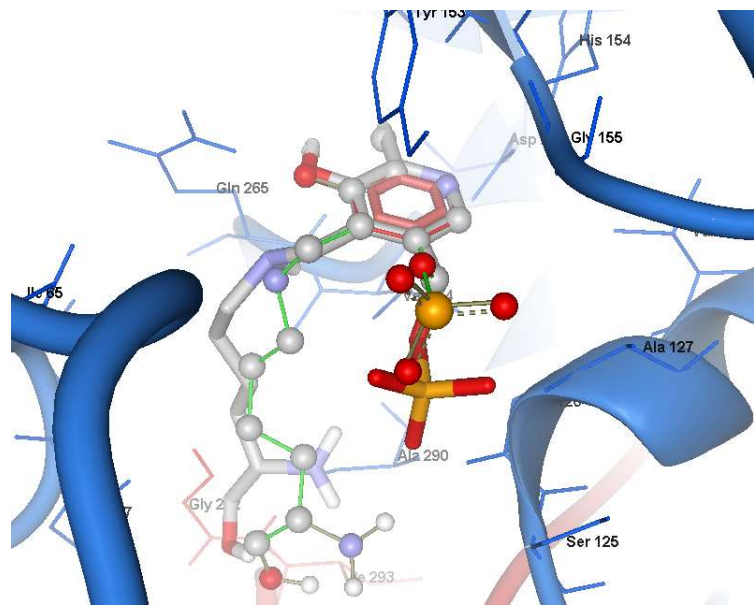


**Figure S16.** Validation of the molecular docking calculation for the *pseudomonas* model. Ligand in the 3r4t crystal structure was reproduced with a RMSD of 1.7 Å. Ligand experimental and calculated conformations are displayed as thick sticks and ball and stick representation respectively.

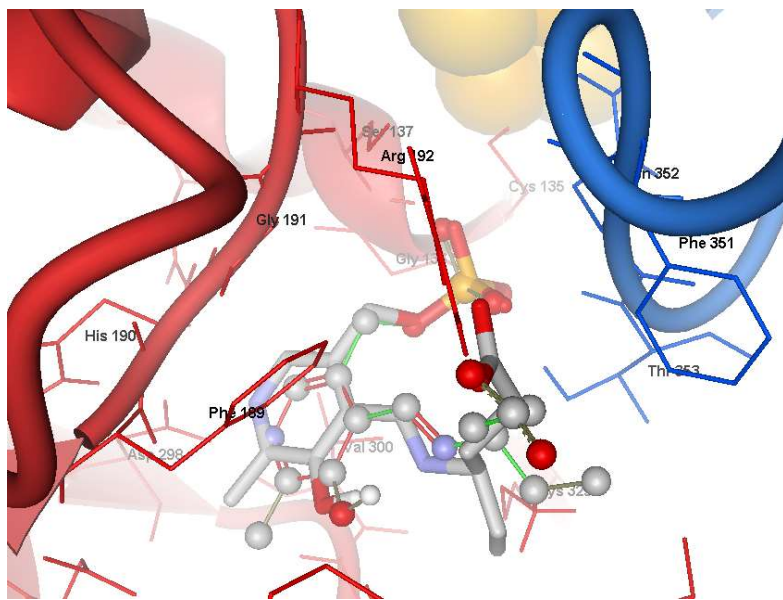


**Figure S17.** Validation of the molecular docking calculation for the *human* model. Ligand in the 1ohw crystal structure was reproduced with a RMSD of 1.3 Å. Ligand experimental and calculated conformations are displayed as thick sticks and ball and stick representation respectively.

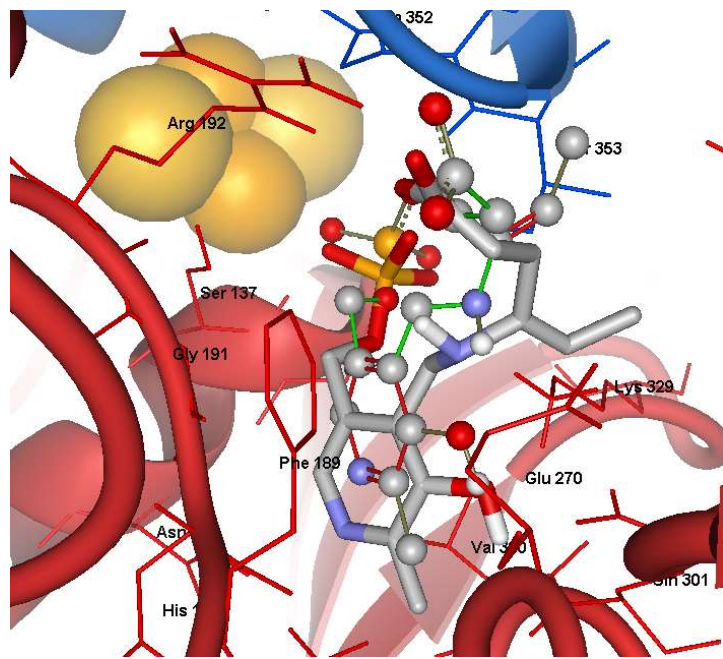
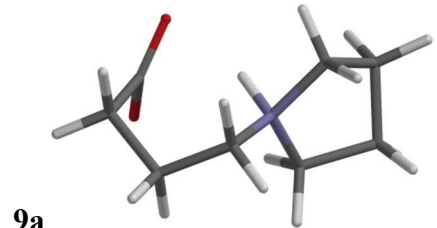
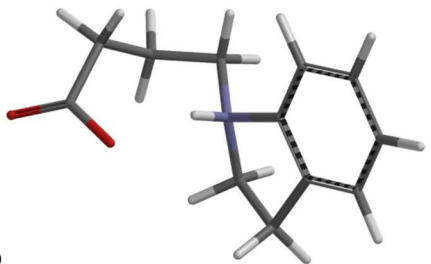


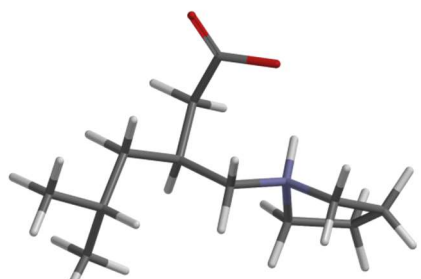
**Figure S18.** Validation of the molecular docking calculation for the *human* model. Ligand in the 1ohy crystal structure was reproduced with a RMSD of 1.8 Å. Ligand experimental and calculated conformations are displayed as thick sticks and ball and stick representation respectively.



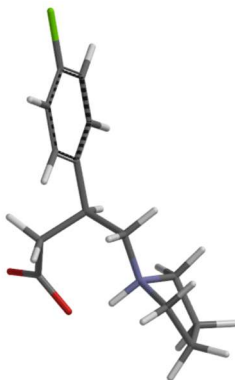
9a



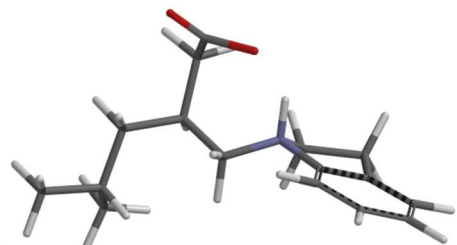
9b



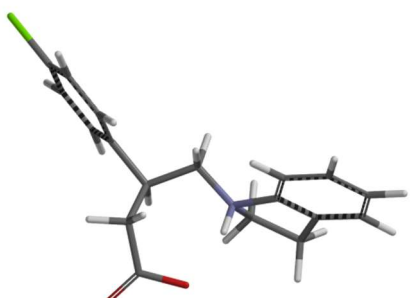
18a



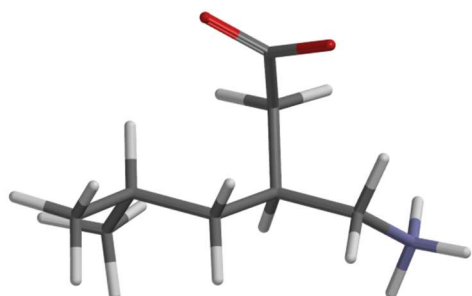
19a



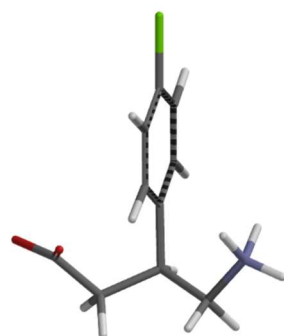
20b



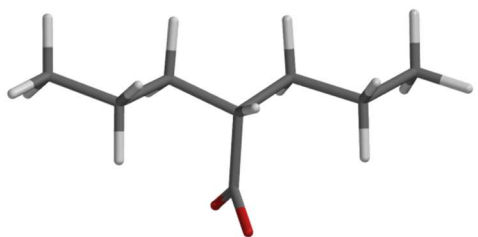
21b



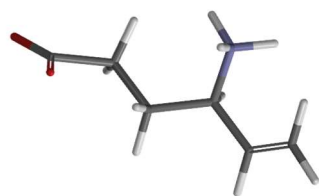
Pregabalin



Baclofen

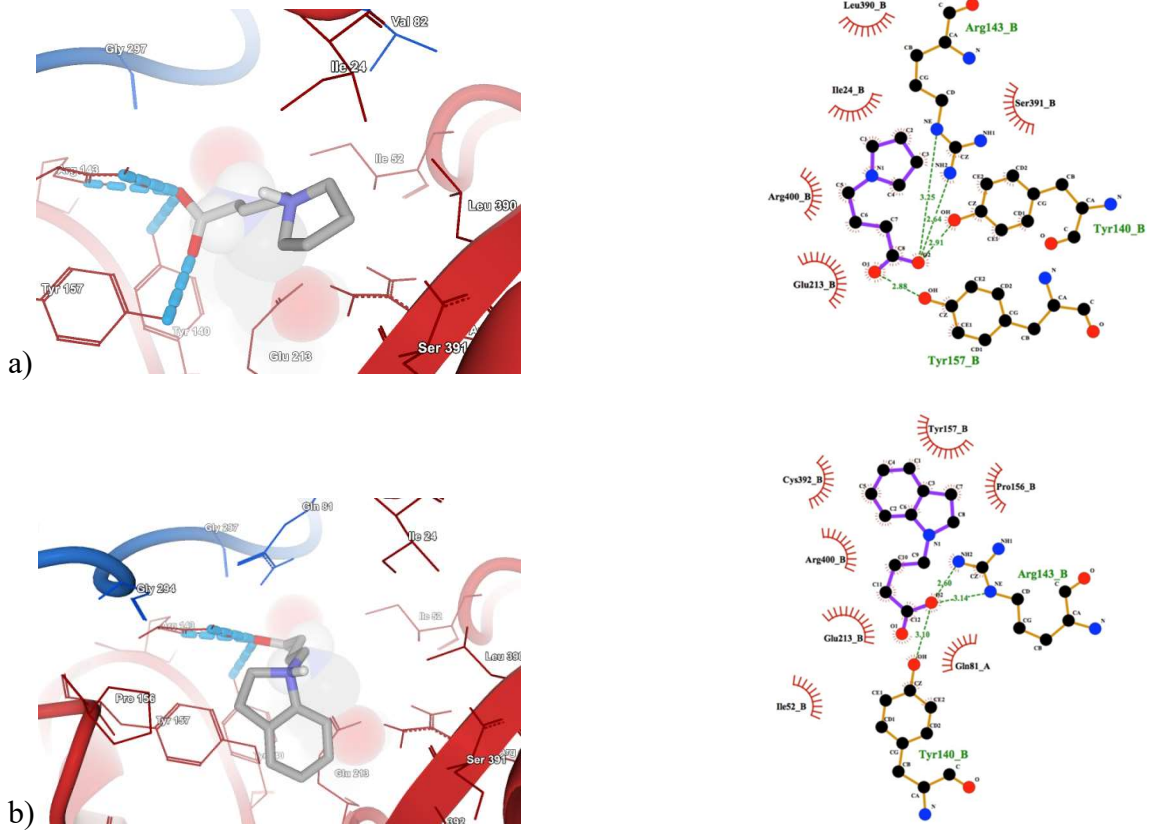


**Valproate**

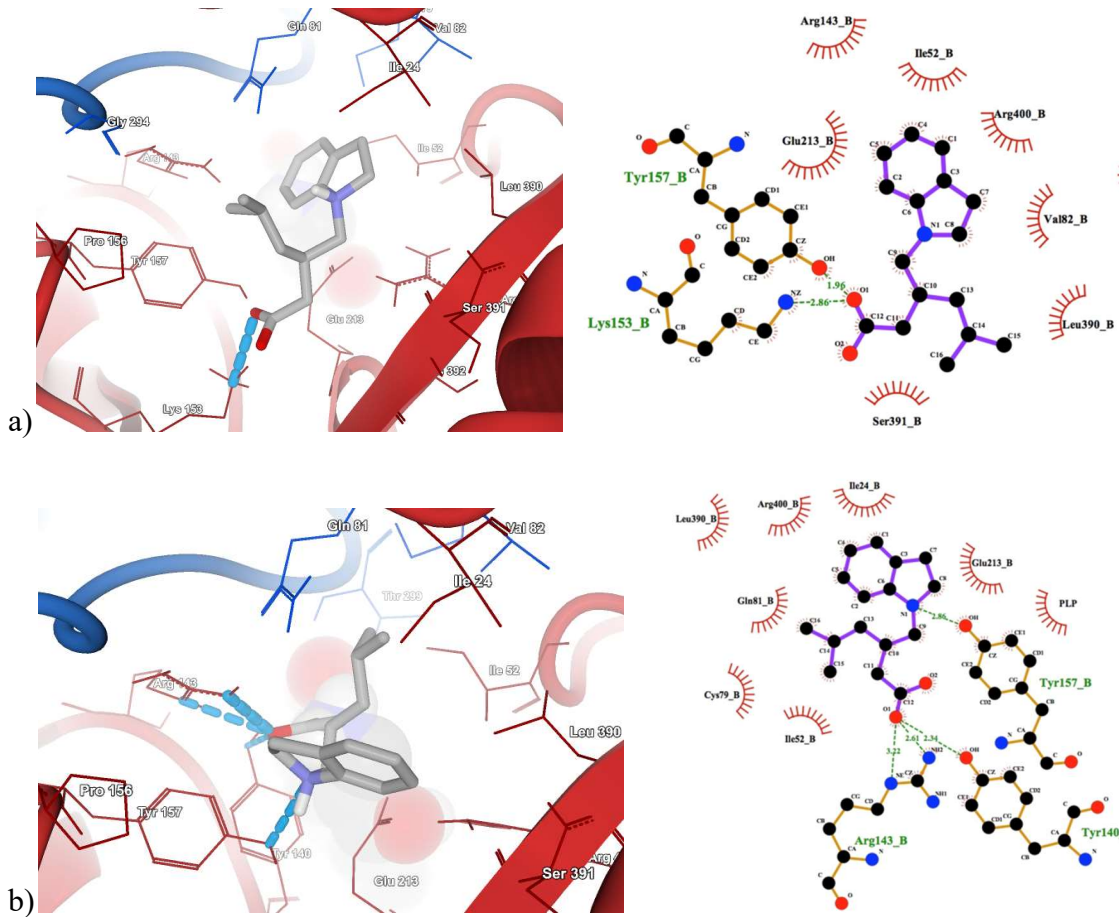


**Vigabatrin**

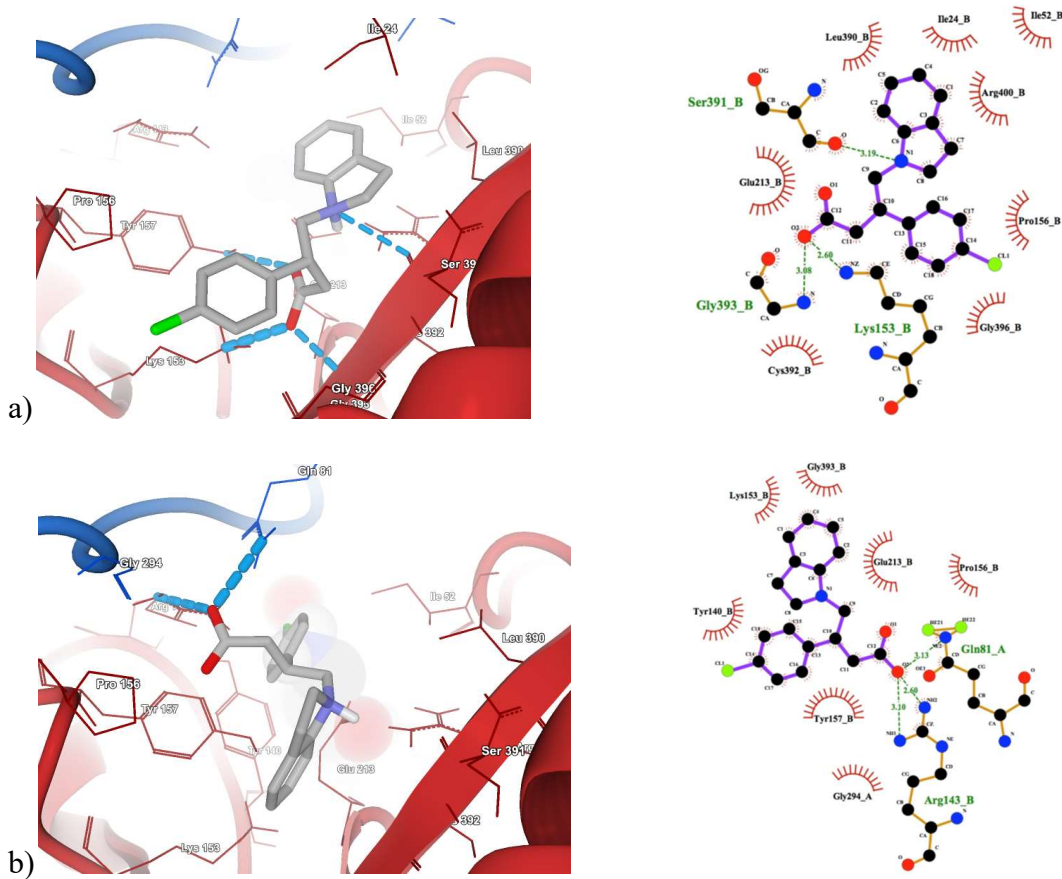
**Figure S19.** Optimized structures of all GABA analogues **9a**, **9b**, **(S)-18a**, **(S)-19a**, **(S)-20b**, **(S)-21b**, Baclofen, Pregabalin, Valproate and Vigabatrin molecules.



**Figure S20.** a) **9a** hydrogen bond interactions (blue dashed lines) with pseudomonas GABA-AT in a 3D and 2D representation. b) **9b** hydrogen bond interactions (blue dashed lines) with pseudomonas GABA-AT. PLP prosthetic group is showed as spacefill model. The images were made with Molegro and LigPlot programs.



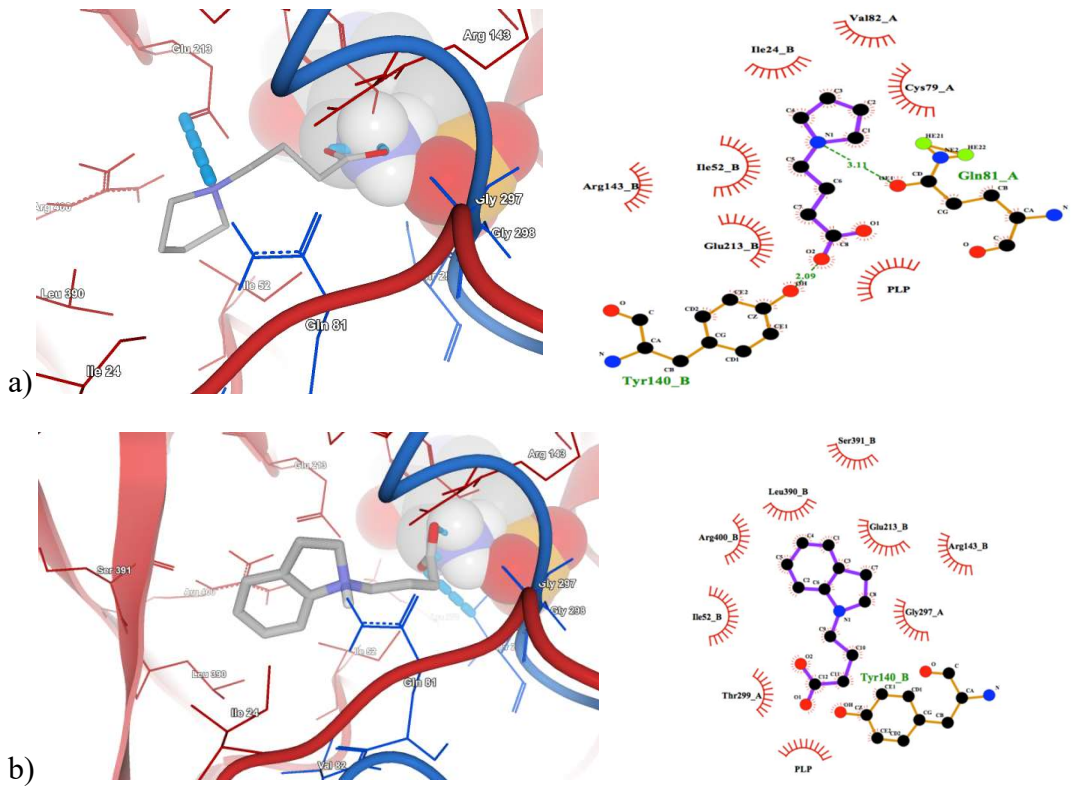
**Figure S21.** a) (*R*)-20b hydrogen bond interactions (blue dashed lines) with pseudomonas GABA-AT in a 3D and 2D representation. b) (*S*)-20b hydrogen bond interactions (blue dashed lines) with pseudomonas GABA-AT. PLP prosthetic group is showed as spacefill model. The images were made with Molegro and LigPlot programs.



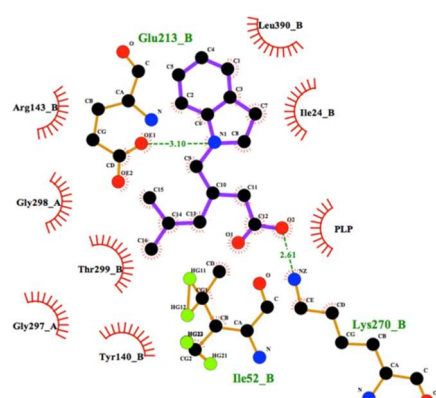
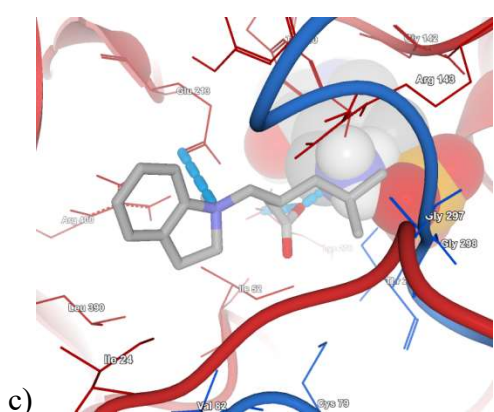
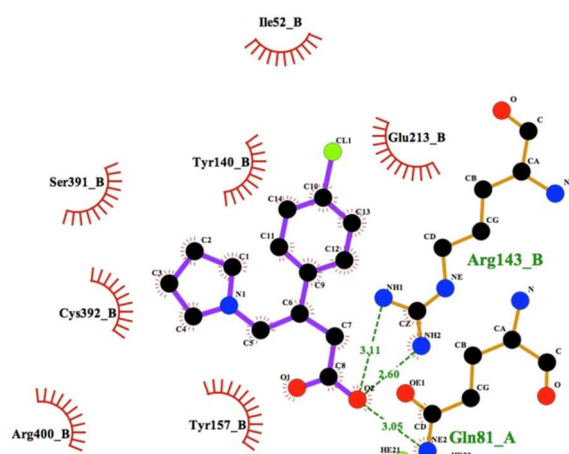
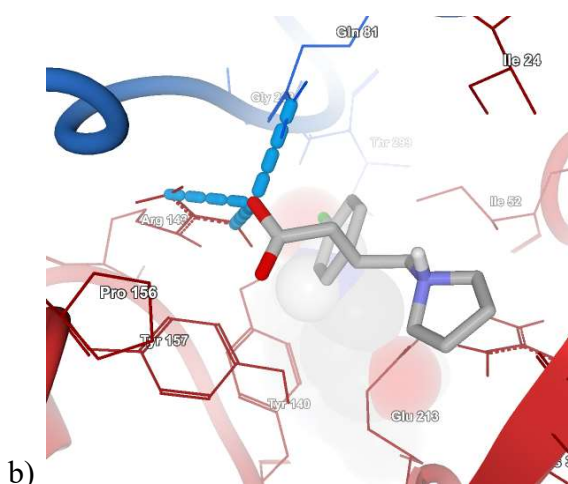
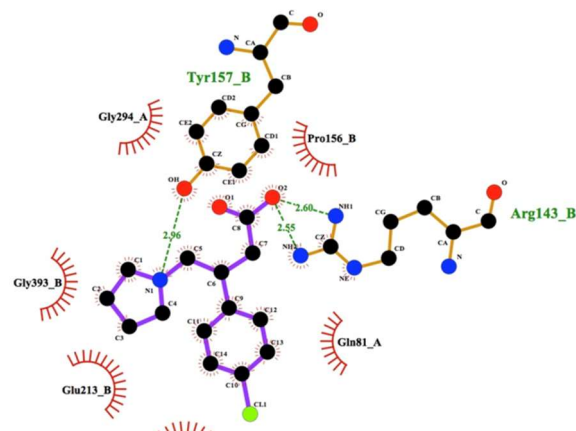
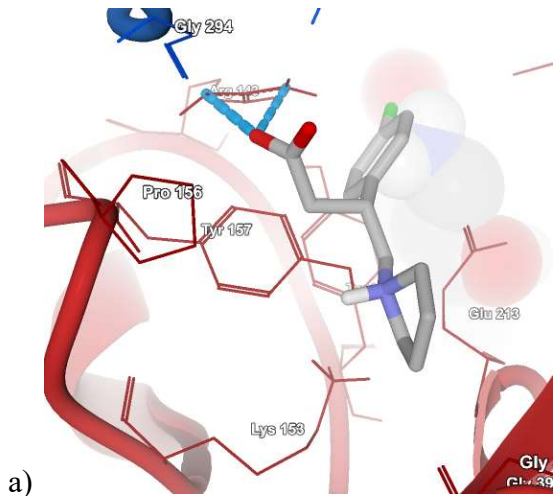
**Figure S22.** a) (*R*)-21b hydrogen bond interactions (blue dashed lines) with *pseudomonas* GABA-AT in a 3D and 2D representation. b) (*S*)-21b hydrogen bond interactions (blue dashed lines) with *pseudomonas* GABA-AT. PLP prosthetic group is showed as spacefill model. The images were made with Molegro and LigPlot programs.

**Table S1.** Energy interactions values obtained from the docking calculations of all GABA derivatives and *pseudomonas* GABA-AT model. All the values are in kcal/mol.

Ligand	MolDock Score	Electro	HBond	Internal	LE
<b>9a</b>	-69.41	-2.39	-8.82	-2.17	-6.31
<b>9b</b>	-80.05	-1.13	-6.78	4.17	-5.34
<b>(R)-18a</b>	-71.30	-4.51	-0.08	-9.08	-4.75
<b>(S)-18a</b>	-82.63	-8.15	-6.96	-4.60	-5.51
<b>(R)-19a</b>	-27.88	-5.49	-1.97	-1.95	-1.55
<b>(S)-19a</b>	-91.07	-5.27	-6.65	-1.46	-5.06
<b>(R)-20b</b>	-81.00	-1.65	-5.55	1.87	-4.26
<b>(S)-20b</b>	-89.51	-6.91	-0.42	-2.89	-4.71
<b>(R)-21b</b>	-96.82	-4.44	-4.75	5.13	-4.40
<b>(S)-21b</b>	-102.18	-6.99	-6.50	1.64	-4.65



**Figure S23.** a) **9a** hydrogen bond interactions (blue dashed lines) with *human GABA-AT* in a 3D and 2D representation. b) **9b** hydrogen bond interactions (blue dashed lines) with *human GABA-AT*. PLP prosthetic group is showed as spacefill model. The images were made with Molegro and LigPlot programs.



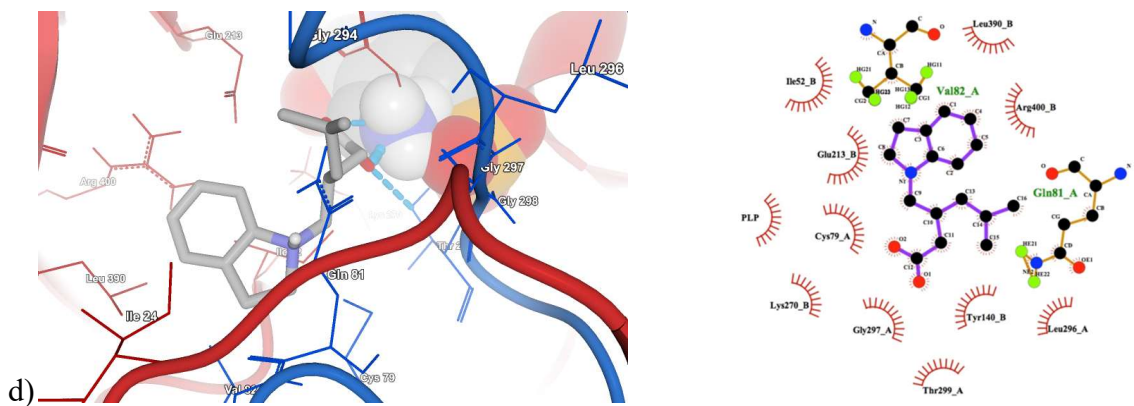


**Figure S24.** a) (*R*)-**18a** hydrogen bond interactions (blue dashed lines) with *human GABA-AT*. b) (*S*)-**18a** hydrogen bond interactions (blue dashed lines) with *human GABA-AT*. c) (*R*)-**20b** hydrogen bond interactions (blue dashed lines) with *human GABA-AT* in a 3D and 2D representation. d) (*S*)-**20b** hydrogen bond interactions (blue dashed lines) with *human GABA-AT*. PLP prosthetic group is showed as spacefill model. The images were made with Molegro and LigPlot programs.

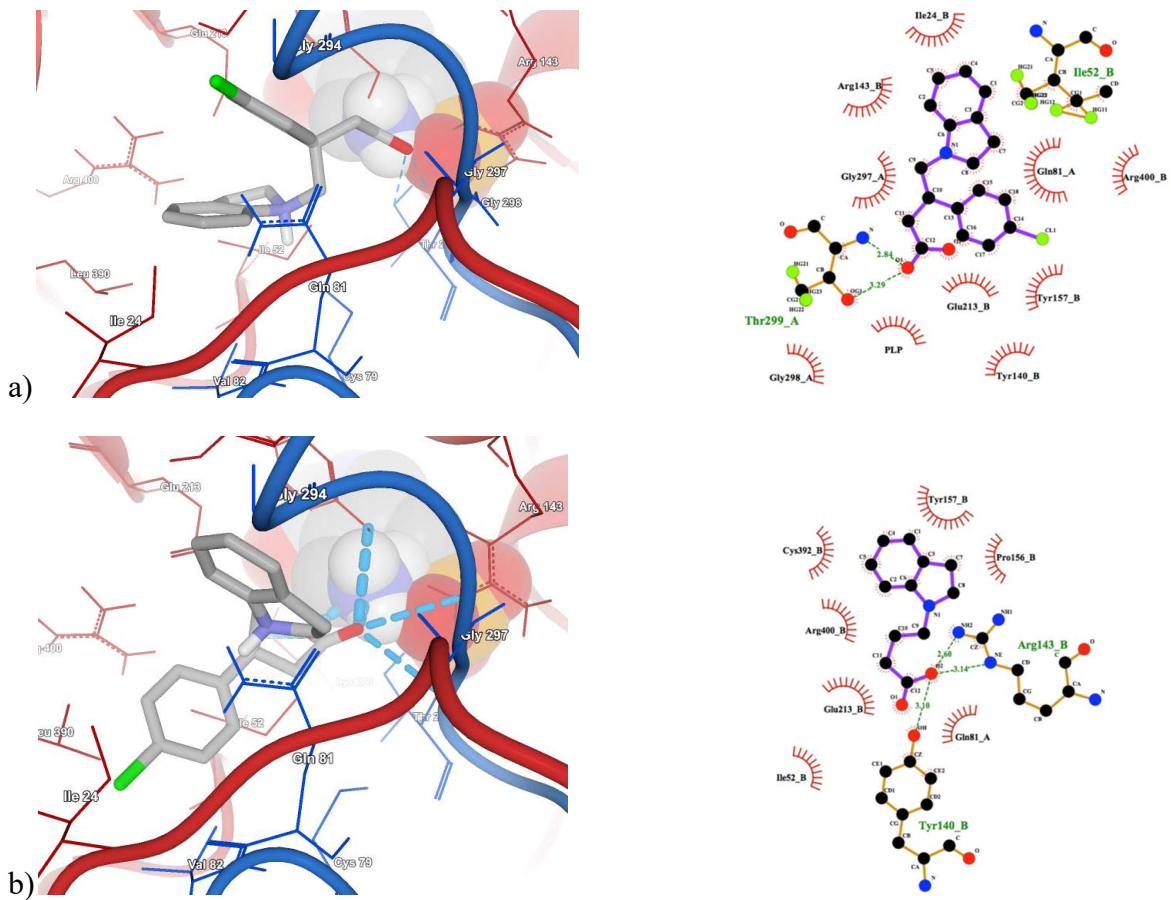


**Figure S25.** a) (*R*)-21b hydrogen bond interactions (blue dashed lines) with *human GABA-AT* in a 3D and 2D representation. b) (*S*)-21b hydrogen bond interactions (blue dashed lines) with *human GABA-AT*. PLP prosthetic group is showed as spacefill model. The images were made with Molegro and LigPlot programs.

**Table S2.** Energy interactions values obtained from the docking calculations of all GABA derivatives and *human* GABA-AT model. All the values are in kcal/mol.

Ligand	MolDock Score	Electro	HBond	Internal	LE
<b>9a</b>	-74.12	-2.31	-0.58	0.57	-6.74
<b>9b</b>	-91.25	-4.18	2.53	3.22	-6.08
<b>(R)-18a</b>	-76.06	-4.82	3.26	-3.15	-5.07
<b>(S)-18a</b>	-78.72	-5.35	-4.59	-6.57	-5.25
<b>(R)-19a</b>	-108.12	-5.32	4.23	3.721	-6.01
<b>(S)-19a</b>	-111.73	-1.97	-8.95	0.78	-6.21
<b>(R)-20b</b>	-80.93	-7.00	-4.94	1.72	-4.26
<b>(S)-20b</b>	-84.63	-0.61	-0.29	-2.00	-4.45
<b>(R)-21b</b>	-98.09	-0.94	0.42	-1.66	-4.46
<b>(S)-21b</b>	-21.54	-5.56	-5.72	6.96	-0.98

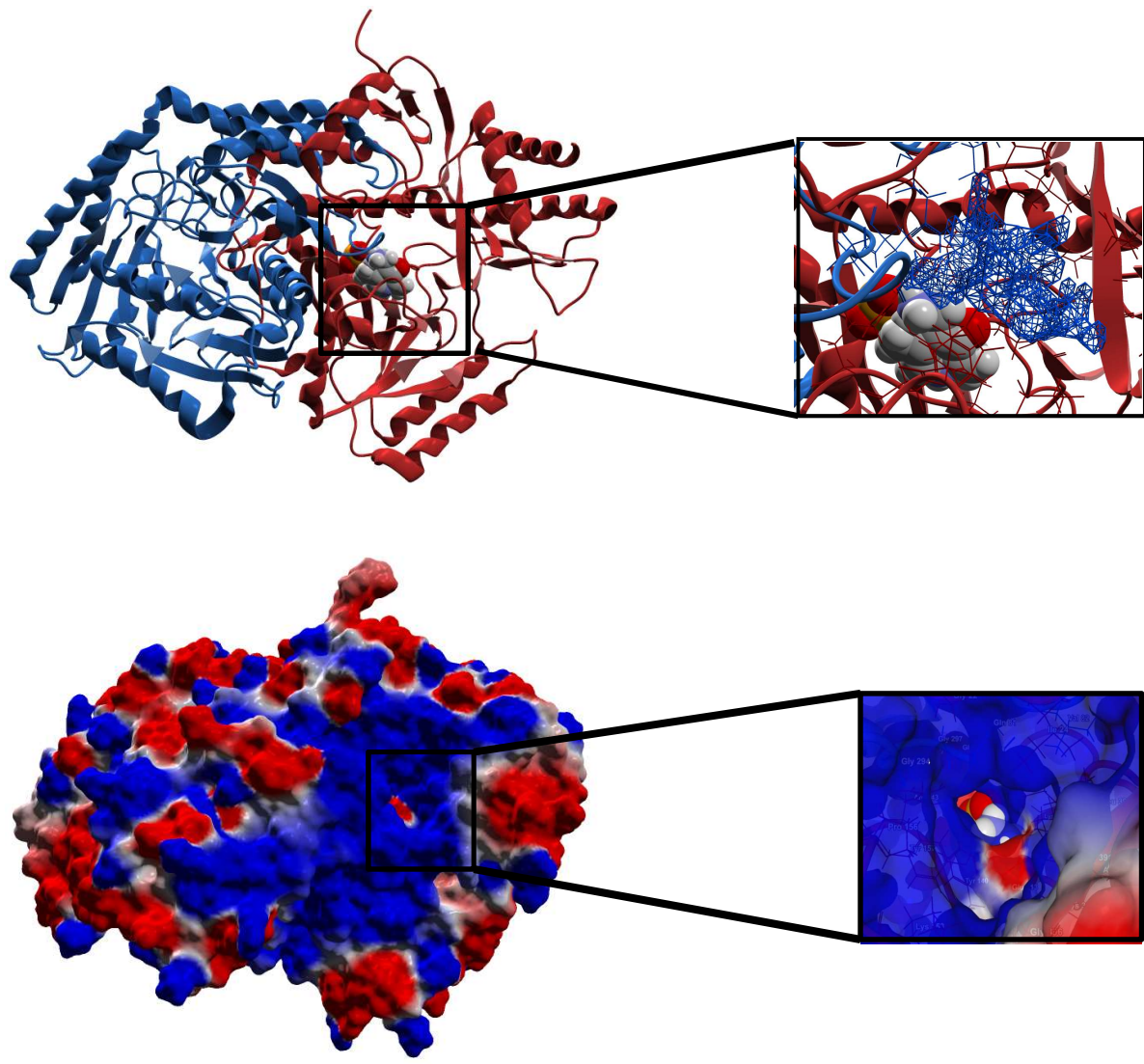


**Figure S26.** Homology model of *Pseudomonas* GABA-AT. The active site and protein cavity (blue color) is displayed. Electrostatic potential map of *Pseudomonas* GABA-AT. Blue, red and white colors represent regions with positive, negative and neutral electrostatic potential value, respectively. PLP prosthetic group is shown as spacefill model.

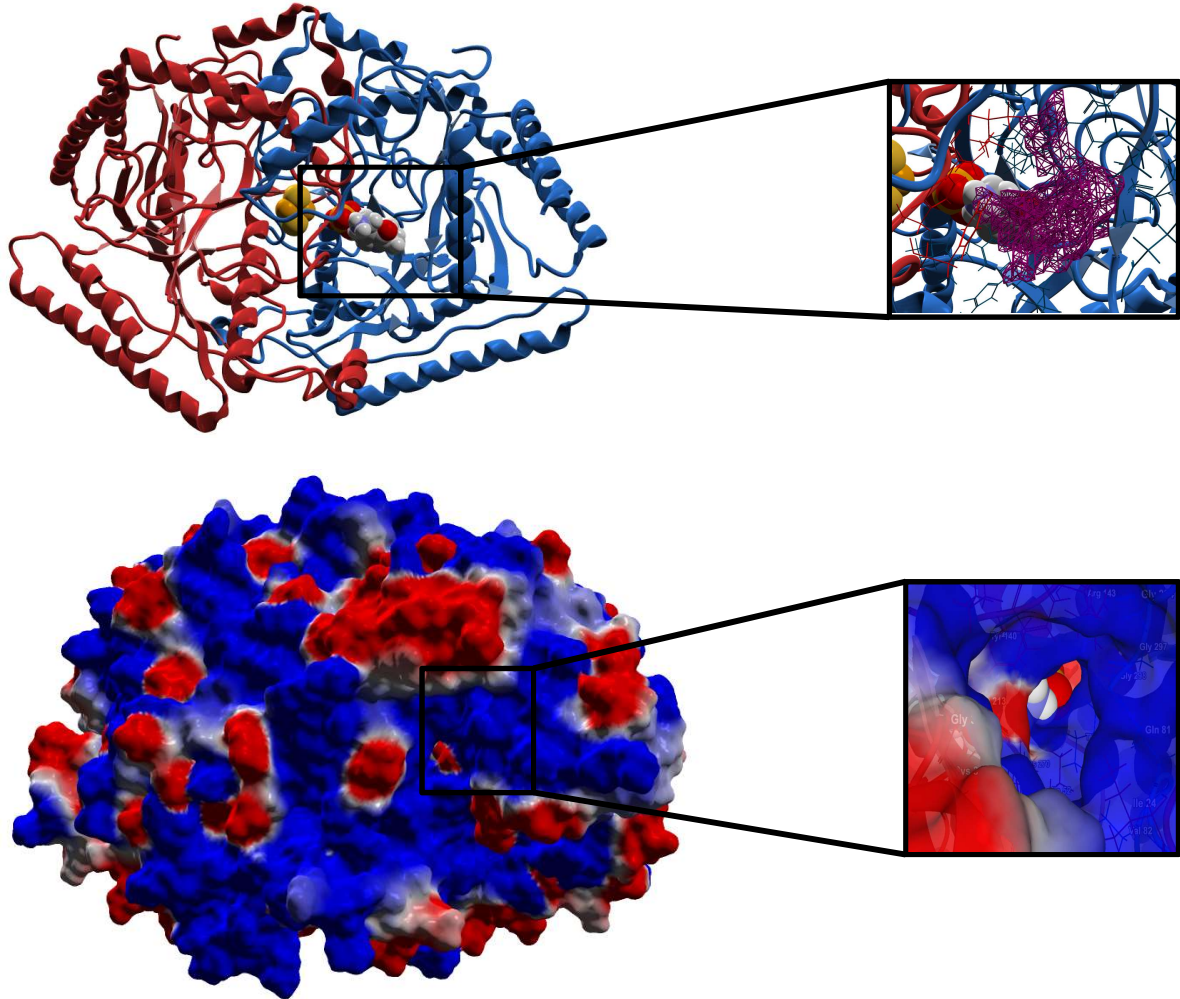


**Figure S27.** Homology model of human GABA-AT, the active site and protein cavity (purple color) is displayed. Electrostatic potential map of human GABA-AT. Blue, red and white colors represent regions with positive, negative and neutral electrostatic potential value, respectively. PLP prosthetic group and Fe<sub>2</sub>/S<sub>2</sub> cluster are shown as spacefill model.